A numerical analysis on forming limits during spiral and concentric single point incremental forming

2017 IOP Conf. Ser.: Mater. Sci. Eng. 164 012009

(http://iopscience.iop.org/1757-899X/164/1/012009)

A numerical analysis on forming limits during spiral and concentric single point incremental forming

M L Gipiela[1], V Amauri[1], C Nikhare[2, 4] and P V P Marcondes[3]
[1]Faculty of Technology – SENAI – CIC, National Service for Industrial Apprenticeship in Paraná, 298 Senador Accioly Filho Street, Curitiba, 81310-000, Brazil
[2] Mechanical Engineering, The Pennsylvania State University, Erie, PA-16563, USA
[3] Graduate Program in Mechanical Engineering - PPGEM, Federal University of Paraná, 210 Coronel Francisco H. dos Santos Avenue, Curitiba, 81531-990, Brazil

Email: cpn10@psu.edu

Abstract. Sheet metal forming is one of the major manufacturing industries, which are building numerous parts for aerospace, automotive and medical industry. Due to the high demand in vehicle industry and environmental regulations on less fuel consumption on other hand, researchers are innovating new methods to build these parts with energy efficient sheet metal forming process instead of conventionally used punch and die to form the parts to achieve the lightweight parts. One of the most recognized manufacturing process in this category is Single Point Incremental Forming (SPIF). SPIF is the die-less sheet metal forming process in which the single point tool incrementally forces any single point of sheet metal at any process time to plastic deformation zone. In the present work, finite element method (FEM) is applied to analyze the forming limits of high strength low alloy steel formed by single point incremental forming (SPIF) by spiral and concentric tool path. SPIF numerical simulations were model with 24 and 29 mm cup depth, and the results were compare with Nakajima results obtained by experiments and FEM. It was found that the cup formed with Nakajima tool failed at 24 mm while cups formed by SPIF surpassed the limit for both depths with both profiles. It was also notice that the strain achieved in concentric profile are lower than that in spiral profile.

1. Introduction

The sheet metal forming industry often use different forming methods which are based on die and punch geometry to manufacture automotive parts. These methods are usually for mass production but when small series or prototypes are required, conventional forming processes can be replaced by new manufacture methods in order to decrease the final costs [1]. In this context, the incremental sheet forming (ISF) processes can replace some of classical sheet metal forming [2].

ISF is a low cost forming process and its use is growing for rapid prototyping, biomechanics and small batch production of sheet metal parts. Considering the following comprehensive market for the ISF technology: small batches of automotive parts, prostheses of biocompatible materials and complex geometries formed from small thickness sheets, it is clear that the ISF is a manufacturing process that needs to be studied [3].

The ISF consists on deform metal blanks by the move of a ball nose punch (spherical) over a blank properly steady in a blank holder [4]. The single point incremental forming (SPIF) is one technique of ISF. In the SPIF, the sheet is held in position with the help of the blank holder which is fixed in a particular position. A simple geometry tool, fixed to the CNC tool is moved along the surface and metal is formed [5]. The principle of the process is shown in Figure 1.

The SPIF depends on a properly programmed path using Computerized Numerical Control (CNC) technology what allows the tool to form a blank by small deformations during the punch tool move [3].

The range of equipment available to perform the ISF techniques is still very limited [6] and because this, some researchers generally are studying ISF using CNC machines. Furthermore, computer aided manufacturing softwares (CAM) are helpful to set the tool path in three axis of the CNC machine and it also permits to test suitable forming parameters in the experiments with reasonable accuracy from CAD files.

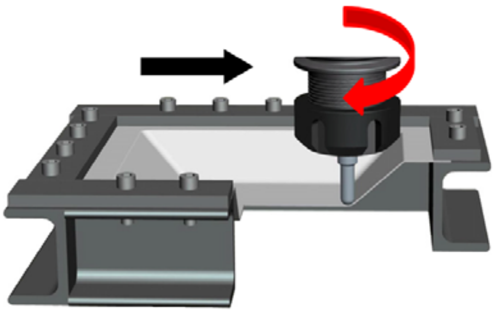

Figure 1. Single Point Incremental Forming principles [4].

Currently, the implementation and understanding of the ISF process focuses on two forms of analysis: numerical and experimental [7]. In the experimental test most of the equipment used for ISF result of the adaptation of CNC machines and running the process with a range of applications in terms of materials and geometries [8]. The use of robots has also been observed in research and it has a great advantage in terms of working area and flexibility. Nevertheless, in addition of error due to the robots joints, it aggravates the IST in terms of final accuracy of the product geometry [9].

Efforts in numerical analysis has been made to develop a better understanding of the fundamental mechanisms involved to predict the materials behavior during the ISF. The modeling of the process by Finite Element Method (FEM) remains a demanding task due a refined mesh element is necessary to achieve convergence and accuracy in the simulations [10].

In the last years, a large number of research related to ISF has been focused on low carbon steels [10-13] and non-ferrous alloys [14-16]. For this reason, there is a great lack of information about process parameters for ferrous materials such as stainless steel, HSS and AHSS steels [3].

Under the circumstances previous mentioned, the main goal of this study is to compare the experimental and numerical results obtained in classical Nakajima test and SPIF numerical results for high strength low alloy steel HSLA440.

2. Material and methodology

The material used for this study is HSLA 440. The experimental true stress-strain curve alongwith the power law is shown in Figure 2. The power law is given in equation 1. The strength coefficient “K” and strain hardening exponent “n” was found by fitting with the experimental curve from 3% to 10% strain and material properties are given in Table 1. For simulation purpose the mix curve was used.

The mix curve is the combination of actual material data upto 3% strain and power law for onwards strain. This curve was used with isotropic hardening law.

$$\sigma = K\varepsilon^{n} \tag{1}$$

where: σ – True stress and ε – True strain

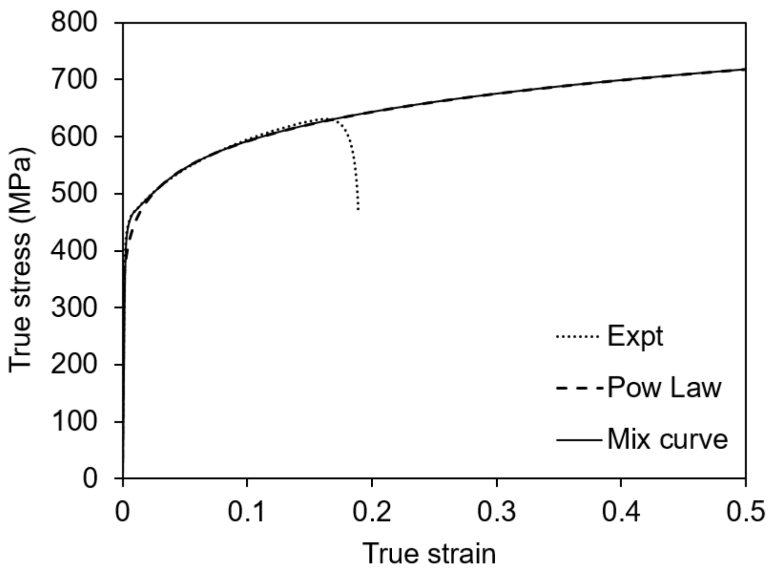

Figure 2. True stress strain curve along with fitted power law.

Table 1. Mechanical properties for HSLA 440.

Yield strength (MPa)	Tensile Strength (MPa)	Total Elongation (%)	K (MPa)	n
437	540	20.8	780	0.12

2.1. Nakajima test and model

The Nakajima experiment was performed to form the hemispherical cup till failure. The Nakajima experimental set up is shown in Figure 3 along with sample dimension. The thickness of the sheet was 1.5 mm. The tests were conducted using 1000 kN capacity hydraulic press. The specimens was oriented with their principal axis along the rolling direction.

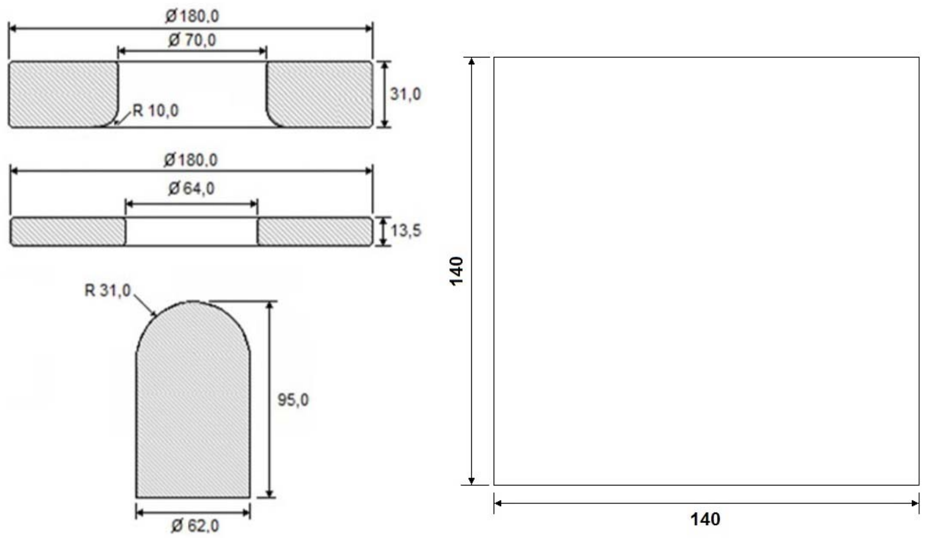

Figure 3. Nakajima test set-up section drawing with dimension in mm (left) and sheet sample for deformation with dimension in mm (right).

Circle grids of 4.2 mm diameter was etched on the specimen. The specimens were mounted with the grid side opposite to the punch and stretched with the punch velocity of 3.99 mm/s ISO VG68 mineral oil was used to reduce the friction between punch and sheet during test. After test, major and minor dimensions of the ellipses, with uniform, localized and fracture deformations, were measured with a Mitutoyo digital caliper.

The Nakajima test was then modeled using ABAQUS/Explicit 6.13-2. The test was investigated with a three-dimensional model approach (Figure 4). The tooling was assumed as a rigid surfaces, while S4R shell elements (4-node quadrilateral, reduced integration) were used to mesh the blank with mesh size of 1.5 mm same as thickness dimension (Figure 4). Full model was used to reduce any discrepancy in the test as single point incremental forming (SPIF) models were needed to done with 3D approach. The average sheet thickness measured experimentally for the HSLA steel was detailed in the model. The true stress-strain data, determined in the tensile tests, was applied to define the material properties using isotropic hardening as explained in material section.

All conditions and process parameters as present in the experimental tests were applied in the numerical model. The interaction between the blank and the rigid bodies were trialed to match the cup height at failure.

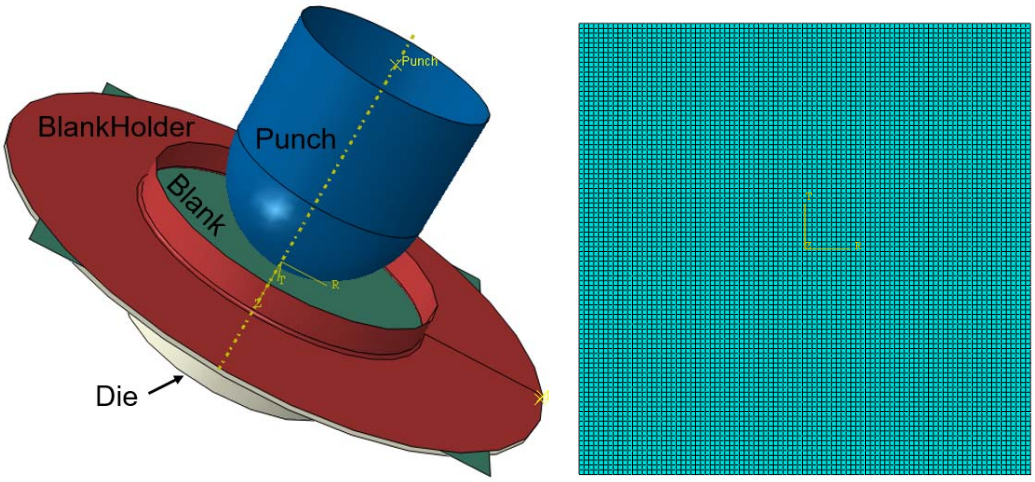

Figure 4. Nakajima test model.

2.2. SPIF models

To model the SPIF the punch was replaced by a 8 mm diameter hemispherical pin. The model is shown in Figure 5. In this paper two profiles were considered to model the SPIF a) spiral profile and b) concentric profile. The spiral x-y profile to create a hemispherical cup with 24 mm height is shown in Figure 6a and the z-depth profile is given in Figure 6b. The profile was created from CAM software Edgecam 2014 R2, which considers the z-increment.

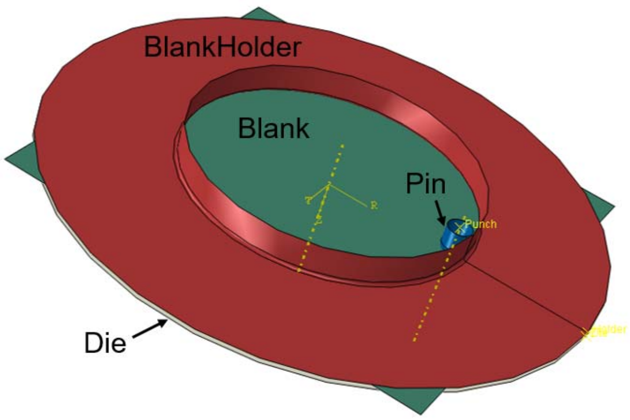

Figure 5. Single point incremental forming model.

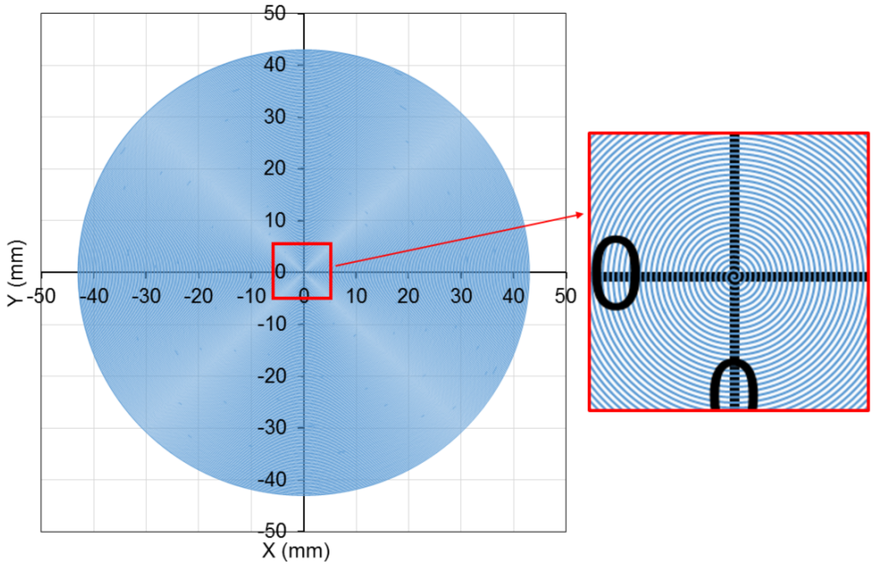

(a)

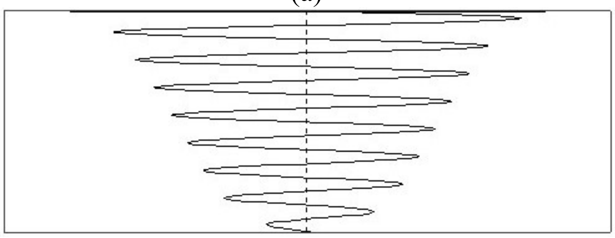

(b)

Figure 6. Single point incremental forming spiral path: (a) x-y profile view and (b) z-depth view.

Similarly the concentric x-y profile is shown in Figure 7a and the z-depth in Figure 7b. In both spiral and concentric SPIF models the tools were assumed as rigid surface and sheet metal as deformable with S4R shell elements. All details are similar to the Nakajima model.

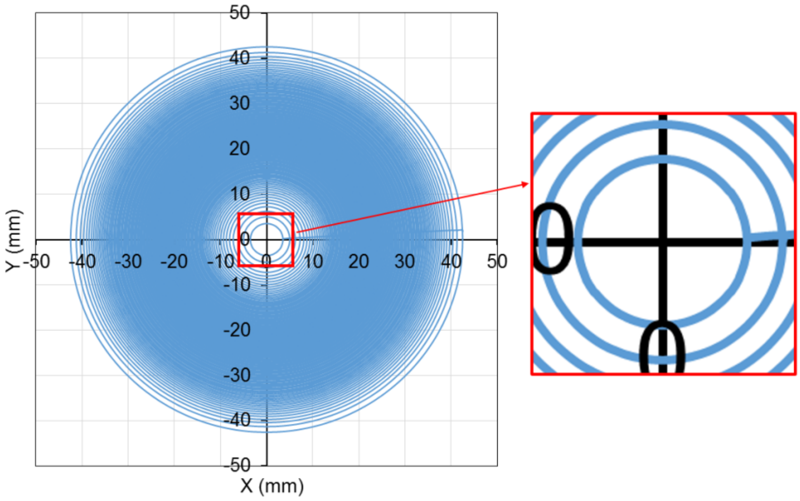

(a)

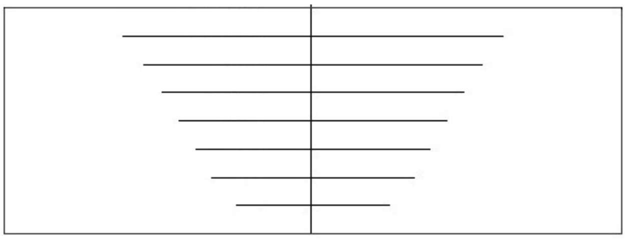

(b)

Figure 7. Single point incremental forming concentric path: (a) x-y profile view and (b) z-depth view.

3. Results and discussion

3.1. Nakajima test and model comparison

The Figure 8 shows the specimen after Nakajima test. The specimen got failure at 24 mm cup depth. A good agreement between experimental and numerical Nakajima results was observed. The results converged in terms of the dome depth and the instability region where the crack occurs. The tested specimen failed at the dome when the punch displaced 24 mm (failure point: engineering minor strain = 0.13 and engineering major strain = 0.37) while in the simulated cup (see Figure 9), the plastic strain distribution reached the instability at the dome when the punch displaced until 24.34 mm. To match the simulation with the experimental cup depth and instability region different coefficient of friction between the punch and blank was tried. The Figure 10 provides the simulated force displacement curve for different friction value. It can be noted that with coefficient of friction of 0.3 the force dropped at 24.34 mm creating the instability in the elements for failure.

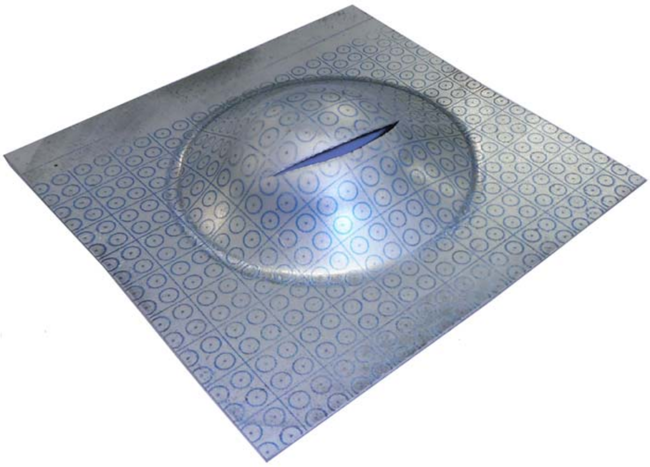

Figure 8. Deformed cup through Nakajima test.

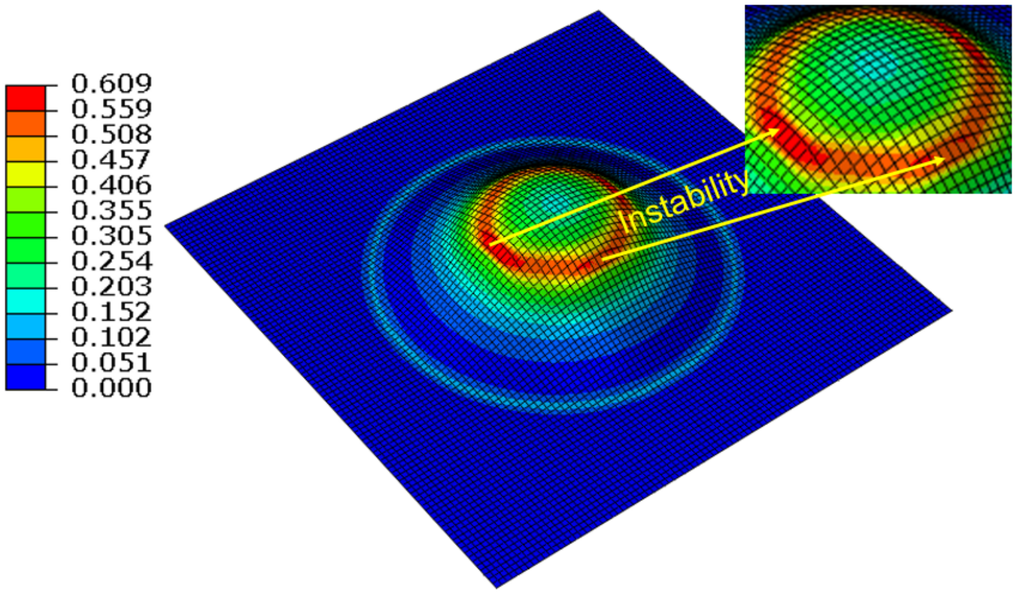

Figure 9. Equivalent plastic strain distribution on cup formed using Nakajima dome test.

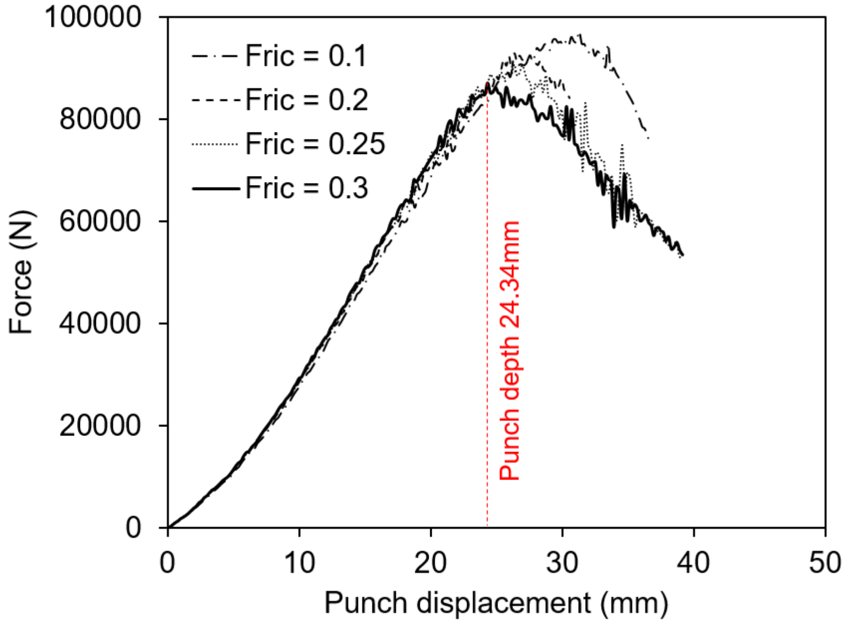

Figure 10. Simulated Force-displacement curve.

3.2. SPIF – Spiral path

Figure 11 and Figure 12 provides the simulated cups by SPIF using spiral path for 24 mm and 29 mm cup height. From equivalent plastic strain contour it can be noted that the cups realizes very high strain of 179.6% for 24 mm cup height and 241% for 29 mm cup height. With these high strain values it can be assumed that these cups are already realized the failure as conventional cups failed at 60.9% equivalent plastic strain (refer Figure 9). However due to unique deformation technique in SPIF that at any time only one point gets deformed and thus can sustain higher strain before failure.

IOP Conf. Series: Materials Science and Engineering **164** (2017) 012009 doi:10.1088/1757-899X/164/1/012009

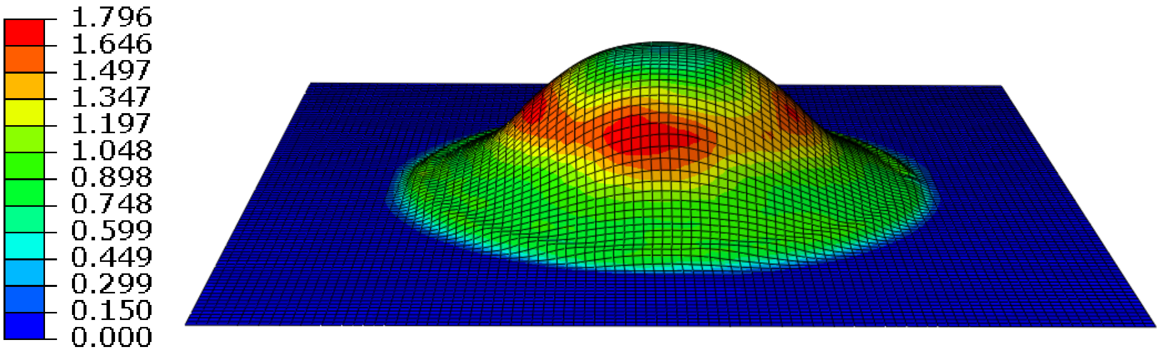

Figure 11. Equivalent plastic strain distribution on 24mm height cup formed using single point incremental forming with spiral path.

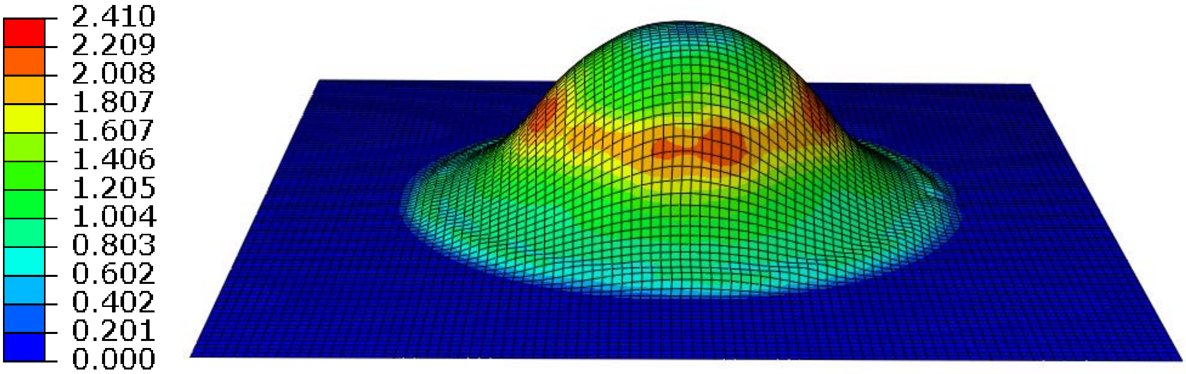

Figure 12. Equivalent plastic strain distribution on 29mm height cup formed using single point incremental forming with spiral path.

3.3. SPIF – Concentric path

Similarly, Figure 13 and Figure 14 provides the simulated cups by SPIF using concentric profiles. It can be observed that these cups also realizes the higher strain of 182.4% and 242% for 24 and 29 mm cup depth. Similar prediction can be made that these cups could have realized failure if they would have been deformed using conventional method.

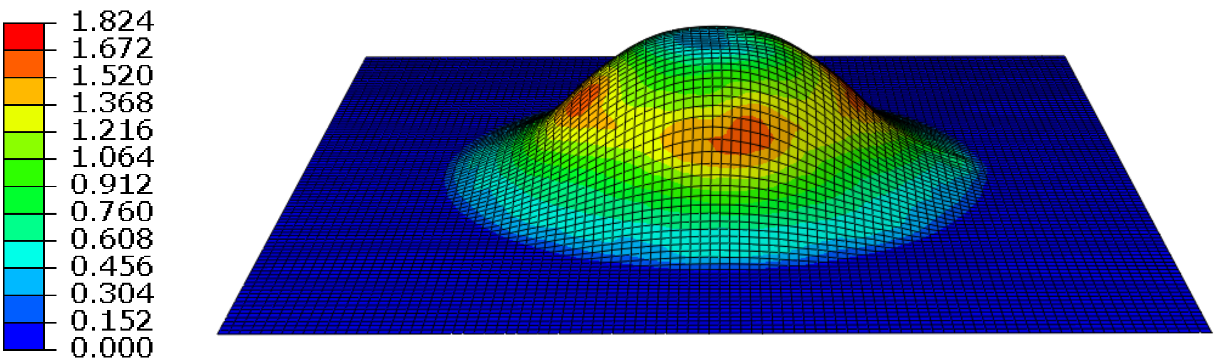

Figure 13. Equivalent plastic strain distribution on 24mm height cup formed using single point incremental forming with concentric path.

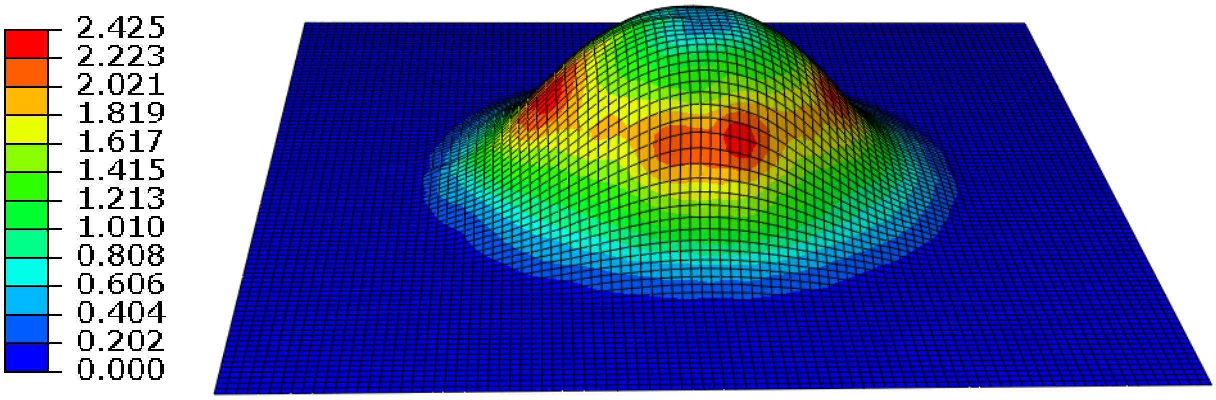

Figure 14. Equivalent plastic strain distribution on 29mm height cup formed using single point incremental forming with concentric path.

3.4. Process comparison

To understand the forces on pin during SPIF, the force with respect to the process time was plotted in each axis. It was found that the forces were similar with both spiral and concentric profile SPIF process in all x, y and z axis (Figure 15-17).

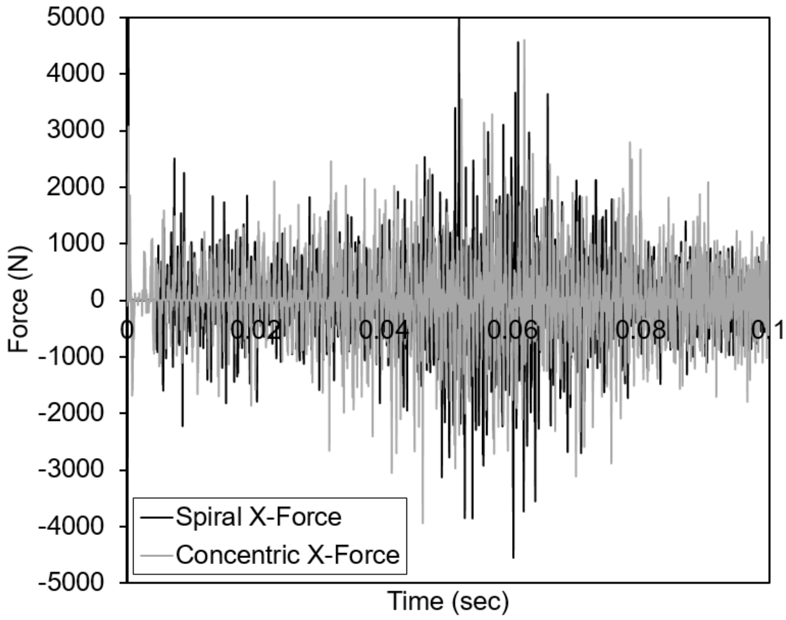

Figure 15. X-axis force with respect to time for 29 mm cup depth.

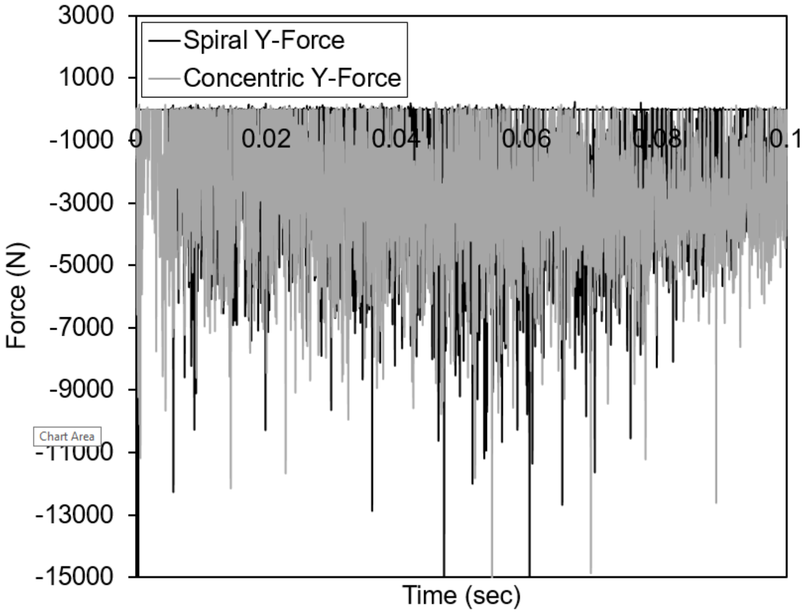

Figure 16. Y – axis force with respect to time for 29 mm cup depth.

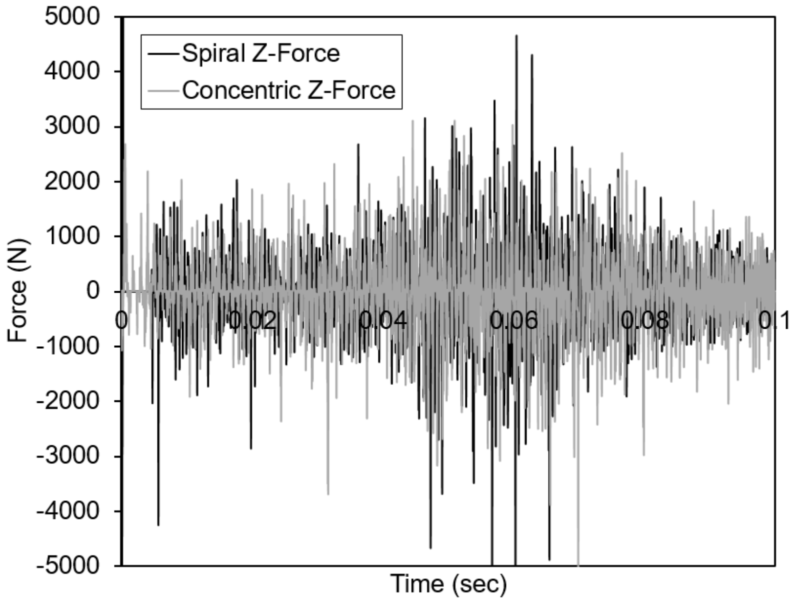

Figure 17. Z – axis force with respect to time for 29 mm cup depth.

Further the critical elements strain paths were plotted in all simulated cups, i.e., Nakajima model, SPIF – Spiral with 24 and 29 mm cup depth, and SPIF – Concentric with 24 and 29 mm cup depth alongwith the failure point from Nakajima test (0.13, 0.37). In addition the literature [17] forming and fracture limit curve for HSLA steel was plotted. It can be seen that the Nakajima test failure point and the simulated instability point matches with the literature forming limit curve.

However as it concluded in previous literature [18] that the failure in SPIF will not be able to predict through conventional forming limit curve and thus fracture limit curve is needed. As can be seen that the strain paths from the SPIF simulated cups with both spiral and concentric profiles for 24 and 29 mm depth could not realized the failure and that they can deform more for further higher depths. It was also observed that for similar depths the spiral profile provides higher major strain value than the concentric profile and would be more prone to failure than the concentric profile for higher depths. This can also be observed in Figure 19 which provides the flow of engineering major strain with respect to the process time for the critical element. Thus concentric profile would be preferred to reach more formability.

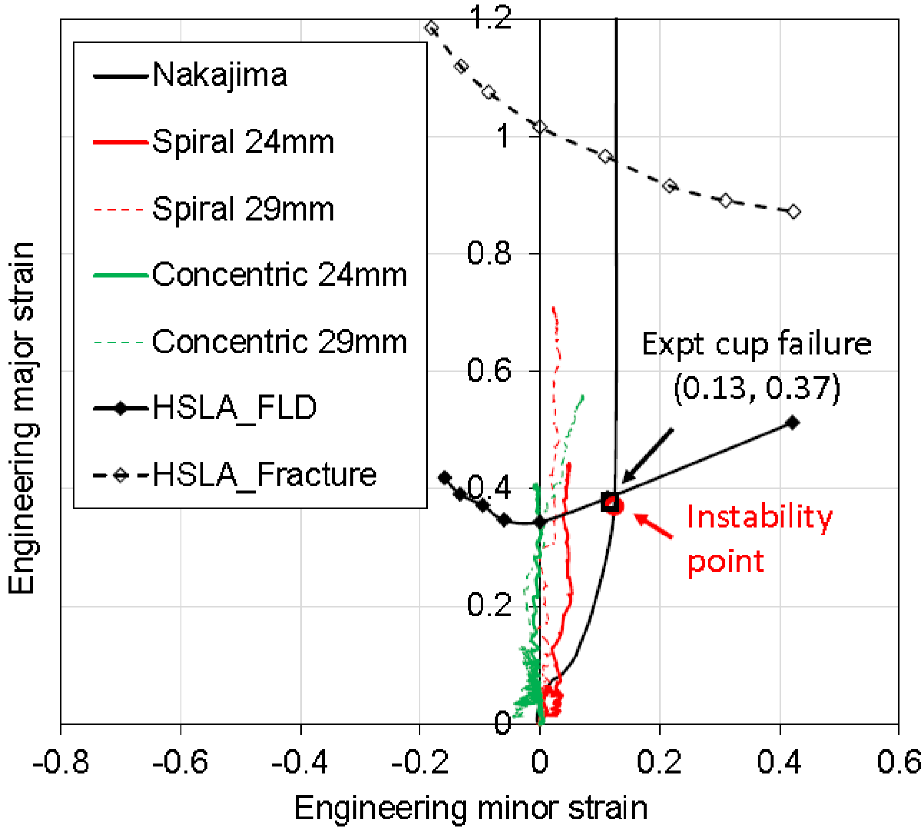

Figure 18. Strain path and forming limits.

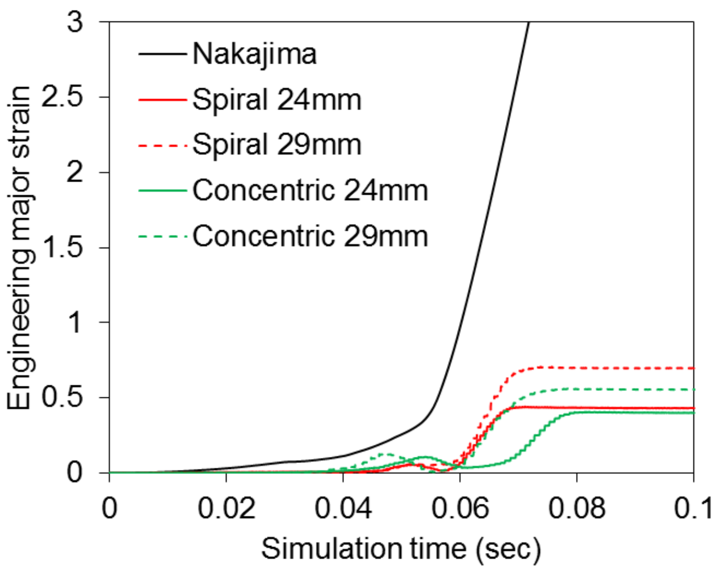

Figure 19. Engineering major strain with respect to simulation time.

4. Conclusion

In this paper the formability and the limits of a hemispherical cups formed by single point incremental forming was studied. For this, the Nakajima test was performed and further modeled the test in ABAQUS. It was observed that the prediction of formability and forming limits was in good agreement with the test. With strain path the deviation was right at the limit curve and thus validates the model. Further single point incremental forming models were prepared and simulated for spiral and concentric path for 24 and 29 mm cup depth. As discussed in previous literature the forming limit curve doesn't realize the failure and thus fracture limit is needed. After plotting the critical element strain path it was observed that both 29 mm cups with spiral and concentric profiles are much below the fracture limit curve and can go further for higher depth. After comparison between the spiral and concentric profile cups for same depth it was found that the concentric profile cup strain path is lower than the spiral profile cup and would realize the failure after spiral profile cup with higher depth. Thus it can be concluded that the formability can be achieved higher in single point incremental forming with concentric profile.

Acknowledgements

The authors would like to thank the ArcelorMittal S. A. by providing HSLA440 blank and SENAI-PR – Faculdade de Tecnologia – Curitiba – Brazil, UFPR – Universidade Federal do Paraná – Curitiba – Brazil and The Pennsylvania State University – Erie – USA for all support.

References

[1] Cerro I, Maidagan E, Arana J, Rivero A and Rodríguez P P 2006 Theoretical and experimental analysis of the dieless incremental sheet forming process *Journal of Materials Processing Technology* **177** 404-408
[2] Bambach M, Hirt G and Ames J 2004 Modeling of optimization strategies in the incremental CNC sheet metal forming process *AIP Conference Proceedings 712: Materials Processing and Design: Modeling, Simulation and Applications, NUMIFORM 2004 Proceedings of the 8th International Conference on Numerical Methods in Industrial Forming Processes (Columbus/Ohio, USA)* pp 1969-1974
[3] Cavaler, L C D C 2010 Parâmetros de conformação para a estampagem incremental de chapas de aço inoxidável AISI 304L Tese de Doutorado, Universidade Federal do Rio Grande do Sul *(Porto Alegre/Brasil)* p 152
[4] Ingarao G, Ambrogio G, Gagliardi F and Lorenzo R D 2012 Sustainability point of view on sheet metal forming operations: material wasting and energy consumption in incremental forming and stamping processes *Journal of Cleaner Production* **29-30** 255-268
[5] Khare U and Pandagale M 2014 A review of fundamentals and advancement in incremental sheet metal forming *IOSR Journal of Mechanical and Civil Engineering* 42-46
[6] Marabuto S R, Sena J I V, Afonso D, Martins M A B E, Coelho R M, Ferreira J A F, Valente R A F and Sousa R J A 2011 Numerical studies and equipment development for single point incremental forming *The 14th International ESAFORM Conference on Material Forming* 1701-1706
[7] Marabuto S R, Sena J I V, Afonso D, Martins M A B E, Coelho R M, Ferreira J A F, Valente R A F and Sousa R J A 2011 Estampagem incremental: estudo numérico e experimental *Congresso de Métodos Numéricos em Engenharia (Coimbra/Portugal)*
[8] Jeswiet J, Micari F, Hirt G, Bramley A, Duflou J and Allwood J 2005 Asymmetric single point incremental forming of sheet metal *CIRP Annals – Manufacturing Technology* **54** 88-114
[9] Meier H, Dewald O and Zhang J 2005 A new robot-based sheet metal forming process *Proc. Shemet* (Erlangen: Germany Trans Tech Publications Ltd) pp 465-470
[10] Fontanari V, Benedetti M, Bruschi S and Fuganti A 2012 A Numerical and experimental analysis of the single point sheets incremental forming process *15th International Conference on Experimental Mechanics (Porto/Portugal)* pp 1-12

[11] Guzmán C F, Bettaieb A B, Sena J I V, Sousa R A, Habraken A M and Duchêne L 2012 Evaluation of the enhanced assumed strain and assumed natural strain in the SSH3D and RESS3 solid shell elements for single point incremental forming simulation *Key Engineering Materials* **504-506** 913-918
[12] Petek A, Kuzman K and Kopac J 2009 Deformations and forces analysis of single point incremental sheet metal forming *Archieves of Materials Science and Engineering* **35** 107-116
[13] Lora F A and Schaeffer L 2014 Incremental forming process strategy variation analysis through applied strains *Brazilian Journal of Science and Technology* **1**(5) 1-8
[14] Taleb Araghi B, Manco G L, Bambach M and Hirt G 2009 Investigation into a new hybrid forming process: incremental sheet forming combined with stretch forming *CIRP Annals – Manufacturing Technology* **58** 225-228
[15] Kopac J and Kampus Z 2005 Incremental sheet metal forming on CNC milling machine-tool *Journal of Materials Processing Technology* **162-163** 622-628
[16] Pohlak M, Majak J and Küttner R 2007 Incremental sheet forming process modelling – limitation analysis *Journal of Achievements in Materials and Manufacturing Engineering* **22** 67-70
[17] Nikhare C, Hodgson P D and Weiss M 2011 Necking and fracture of advanced high strength steels *Materials Science and Engineering A* **528** 3010-3013
[18] Silva M B, Skjødt Martin, Atkins A G, and Martins P A F 2008 Single-point incremental forming and formability-failure diagrams *Journal of Strain Analysis for Engineering Design* **43** 15-35